Molecular Dynamics Simulation Study of the Negative Hydration Effect in Aqueous Electrolyte Solutions

A. Geiger

Institut für Physikalische Chemie und Elektrochemie der Universität Karlsruhe, Kaiserstraße 12, D-7500 Karlsruhe

Diffusion / Flüssigkeiten / Lösungen / Molekulardynamik

To study the structure breaking effect in aqueous electrolyte solutions (also termed negative hydration), a series of molecular dynamics simulation runs has been carried out. An originally uncharged, nonpolar spherical solute particle ("Xenon") is charged step by step from $q_I = 0.0e$ to $q_I = +0.67e$, $+1.0e$ and $q_I = +2.0e$ (e is the positive elementary charge). At zero charge the occurrence of hydrophobic hydration is observed. The surroundings of the divalent cation also shows marked structuring: the normal "positive" ionic hydration. In an intermediate region of charge (at $q_I \approx 1.0e$) negative hydration is detected, which proves to be a state of minimum order. Structural changes are discussed by using pair and three particle correlation functions. Hydration energies, binding energies and pair interaction energy distributions are determined. The microdynamics is studied by observing the reorientational motion and the self diffusion behaviour of the water molecules in different regions. A zone of increased mobility is located in the vicinity of the ion, which may include the innermost hydration shell. Additionally a system comprising a negatively hydrated anion has also been studied.

1. Introduction

The success of the first computer simulation studies on pure water by Rahman and Stillinger [1 – 4] stimulated the treatment of aqueous solutions along similar lines. Several studies which gave more insight into the mechanisms of hydrophobic hydration were reported recently [5 – 7]. Applying again Rahman and Stillinger's method, the present paper is aimed to investigate the phenomenon of negative hydration (or structure breaking effect), which is produced by certain large mono- and divalent ions in water (but also in a few other liquids like glycerol and ethylene glycol) [8].

One basic experimental observation is the greater fluidity of the aqueous solutions of several salts compared to pure water. On a microscopic scale this increase of fluidity means that the average thermal motions of the water molecules are faster in these solutions than in pure water. In fact, nuclear magnetic relaxation [9] as well as dielectric relaxation [10] experiments showed that there are water molecules in these solutions which have a faster reorientation and self diffusion behaviour than the bulk water molecules.

Concerning the location of these mobile water molecules, Frank and Wen [11] suggested the well-known concentric-shell model of ionic hydration assuming that an innermost region of immobilization is surrounded concentrically by a region of structure breaking. Gurney [12] concluded that for special combinations of ionic size and charge, this region of faster thermal motion may extend up to the immediate vicinity of the ion, extinguishing the inner region of immobilization. He discusses an imaginary experiment, in which a spherical solute, having roughly the size of a water molecule, is placed into water being near its freezing point and in which the charge on this ion is made to vary continuously from a value near zero to a value greater than $+2e$ (where e is the positive elementary charge = $1.6022 \cdot 10^{-19}$ C). At some critical value of the ionic charge, the ordering influence exerted on a water molecule in the first hydration shell by the ion will be comparable to the influence of the surrounding water molecules. Due to this concurrence, energy barriers will be flattened out and thermal motion will break up the local structure, reducing the degree of ordering in the ionic hydration shell. Samoilov [13] essentially came to the same results by considering the translational motion of the water molecules.

Besides this microdynamic behaviour the structure breaking effect of solutes in water shows up in many other properties as well [14]. According to the various methods used to study structural changes in aqueous solutions, a number of different criterions has been applied to classify solutes as structure breaking or structure promoting. But there have been only few attempts to describe the structure changing influence of solutes on the basis of molecular pair correlation functions. This had

Ber. Bunsenges. Phys. Chem. *85*, 52 – 63 (1981) –
0005 – 9021/81/0101 – 0052 $ 02.50/0

been suggested by Hertz [15], considering mainly orientational distribution functions. Stillinger and Ben Naim [16] used an integral over the intermolecular oxygen-hydrogen pair correlation function, representing the excess number of protons in the region surrounding a fixed water molecule. Hertz and coworkers [17] evaluated nuclear magnetic relaxation time measurements to obtain parameters of simple ion-proton model pair distribution functions for various ions. As pointed out by Franks [18], the use of three-particle correlation functions (water-ion-water) would be more appropriate to describe the structural influence of solute particles, but there are only few experimental quantities from which information about these functions can be drawn (e.g. nuclear quadrupolar relaxation [19]*)).

Direct and unambiguous informations about pair correlations in aqueous solutions should be obtainable from diffraction experiments. But until now there are only few systems, where this has been achieved. From neutron scattering experiments – using isotopic substitution methods – Enderby and coworkers [20] extracted correlation functions which describe the structure of Ni^{2+} and Cl^- hydration-shells and which can be easily interpreted. There exists also a number of X-ray diffraction studies on aqueous electrolyte solutions [21], but to interprete these data, detailed models have to be introduced.

During the last years a number of computer simulation studies concerning aqueous electrolyte solutions or small ion-water clusters have been published, mostly Monte-Carlo [22–25], but also molecular dynamics [26–29] calculations. A recent review of this field has been given by Watts [30]. Simple empirical model potentials, as well as potentials derived from quantum mechanical calculations were used. But no systematic investigation concerning the occurrence of the structure breaking effect has been reported.

The present study represents a model experiment with a computer generated liquid, which can not be performed in reality, but which may give a better understanding of the mechanisms causing the phenomenon of negative hydration. It closely follows Gurney's Gedankenexperiment: An originally uncharged, nonpolar spherical solute particle is charged step by step from $q_I = 0.0e$ to $+0.67e$, $+1.0e$, and $q_I = +2.0e$. In the case of zero charge we expect the occurrence of the so-called hydrophobic hydration: water structure promotion in the vicinity of the solute, as already described in Ref. [5]. The surroundings of the divalent cation should also show strong structuring: the usual "positive" ionic hydration. In an intermediate region of charge (at about $q_I = 1.0e$, when using the present ion size) "negative hydration", i.e. the structure breaking effect should be observed. In addition, two supplementary simulation runs have been carried out: One system comprising an anion ($q_I = -1.0e$) in the negative hydration region, as well as one simulation run at increased temperature (with $q_I = +1.0e$).

When investigating these systems, two main questions shall be considered:

1. Of which kind are the occurring structural changes? How can we replace qualitative descriptions like "structure promotion" or "structure breaking" by more quantitative concepts?
2. Where do we find the zone of increased fluidity in the case of negative hydration?

2. Molecular Dynamics Outline

The systems to be studied by the MD technique consist of one spherical solute particle surrounded by 215 water molecules in a cubical box subject to periodic boundary conditions. In a series of simulation runs electrical point charges of different size were added to the center of the solute sphere.

The interaction between the water molecules is given by the ST2-model potential [3–5]. The pair potential describing the interaction between the water molecules and the dissolved ion consists of a Lennard-Jones part $V_{LJ}^{IW}(r_{IW})$ and a Coulomb term $V_{el}^{IW}(r_I, x_W)$

$$V_{IW}(r_I, x_W) = V_{LJ}^{IW}(r_{IW}) + V_e^{IW}(r_I, x_W)$$

r_I is the position vector of the ion center, x_W represents position plus orientation coordinates of water molecule W. The ion-oxygen distance has been denoted by r_{IW} and

$$V_{LJ}^{IW}(r) = 4\varepsilon_{IW}[(\sigma_{IW}/r)^{12} - (\sigma_{IW}/r)^6]$$

$$V_{el}^{IW}(r_I, x_W) = q_I|q_W| \sum_{\alpha=1}^{4} (-1)^\alpha / d_{I\alpha}$$

with q_I the ionic charge and $q_{W\alpha} = (-1)^\alpha \cdot |q_W|$ the partial charges of the ST2 water model [3]. $d_{I\alpha}$ is the distance between the ion center and the charge α on water molecule W. σ_{IW} and ε_{IW} have been derived by combining Xe–Xe-parameters with the ST2-parameters [31, 32]:

$$\sigma_{IW} = 3.7 \text{ Å}, \qquad \varepsilon_{IW} = 0.753 \text{ kJ/mol}.$$

To save computer time when calculating water-water interactions, a cutoff distance $r_c = 7.8$ Å between the oxygens was chosen, beyond which interactions were disregarded. This value corresponds to the third minimum of the pair correlation function $g_{OO}(r)$. A justification for the use of this small value was already given in Ref. [5]: The main interest of this study is directed towards microstructural and microdynamic properties in the immediate vicinity of the solute which are probably less affected by this choice than are the thermodynamic properties. Also, mainly differences between bulk and shell water were investigated, so that for several properties contributions from more distant interacting partners can be expected to cancel out in large measure.

The Coulomb interactions involving the ionic charge are calculated by using the Ewald summation method as described in the central force model study of pure water by Rahman et al. [33]. Due to the summation procedure of the Ewald method and because no counter-ion is present in the system, the ionic charge is counterbalanced by a uniform rigid neutralizing background charge of opposite sign and equal magnitude which gives a small contribution to the total energy of the system but does not influence structure and dynamics. In fact, for one system ($q_I = -1.0e$) a short control simulation run was executed, calculating the ion-water interaction in the minimum

*) The electric field gradients causing relaxation of the ionic nuclei are mainly due to the charge distribution in the hydration shell. They have also been calculated during the present work and will be published separately.

image approximation. Within the statistical errors and fluctuations not significant differences could be observed.

The size of the cubic box which was used in the original pure water simulation [1] (L = 18.626 Å) was not altered, providing a density of 0.0334 particles/Å^3. The mass of the solute ion was fixed to be the xenon mass m = 131.3 atomic units which results in a mass density of 1.03 g/cm^3 for all systems. The computational procedure for the numerical integration of the dynamical equations corresponds to the one described by van Gunsteren et al. [34], applying a procedure called SHAKE [35] to satisfy the constraints of rigid water molecules. The timestep for the integration was $\Delta t = 1.22 \cdot 10^{-15}$ s.

Table 1
Specification of the six MD runs. In each case the density is 0.0334 particles/Å^3, corresponding to 1.03 g/cm^3. Timesteps $\Delta t = 1.22 \cdot 10^{-15}$ s

System	q_I/e	T/K (°C)	E_{tot}^{uncorr} / kJ mol^{-1}	Number of timesteps	Total time interval in ps
I	0.0	293 (20)	−35.13	4562	5.58
II	0.67	297 (24)	−35.34	5490	6.71
III	1.0	292 (19)	−36.45	5662	6.92
IV	2.0	303 (30)	−40.43	4516	5.52
V	−1.0	288 (15)	−37.29	5714	6.98
VI	1.0	321 (48)	−33.52	4396	5.37

Some data characterizing the simulated systems are summarized in Table 1. The total energy was specified in such a way, as to obtain temperatures (calculated from the average total kinetic energy) near room temperature, except for system VI, where a higher temperature was desired. The given total energies E_{tot}^{uncorr} are due to the truncated water interaction potential as described above and are not corrected. Total energy drifts due to cutoff and numerical "noise" were met by momentum rescaling as mentioned in Ref. [5]. The "aging" (equilibration) of the systems, prior to the proper production period, needed 2 to 7 ps, depending on how the system was created.

3. Structure of the Hydration Shell

3.1. Nuclear Distributions

3.1.1. Ion-Water Radial Pair Correlation Functions

The ion-oxygen and ion-hydrogen radial pair correlation functions $g_{IO}(r)$ and $g_{IH}(r)$ are shown in Fig. 1 (here and in the following the uncharged particle will also be termed "ion" for

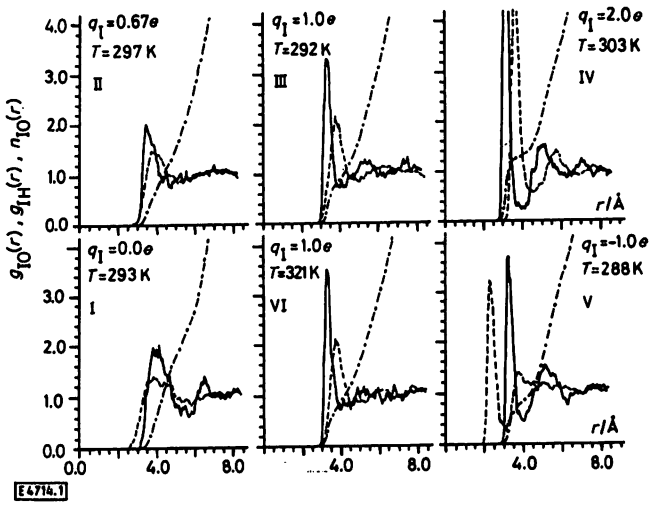

Fig. 1
Ion-oxygen and ion-hydrogen radial pair correlation functions $g_{IO}(r)$ and $g_{IH}(r)$ (full and dashed lines respectively). Dot-dashed lines: running coordination number $n_{IO}(r)$ scaled by a factor of 0.1

abbreviation, considering it as the corresponding limiting case). The arrangement of the individual graphs in Fig. 1 which correspond to the six different systems is such that the cation charge is increasing when proceeding in clockwise direction from the lower left to the upper right corner. Additionally those two systems which differ only in temperature are in the same column. This particular order is conserved in all similar figures which are following.

With increasing ion charge we observe an increased structuring indicated by a clear narrowing and strong increase of the first peak in the pair correlation function. At $q_I = +2.0e$ the height of the maximum reaches 9.0 resp. 4.8 for g_{IO} and g_{IH}. Table 2 gives the position of the first peak and the following minimum for the different systems. In the case of $q_I = 1.0e$ it can be seen that this peak does not change within statistical accuracy when increasing the temperature, whereas other features at larger distances are flattened out. Comparing the monovalent cation and anion we find that the anion pair correlation functions are more structured although both ions differ only by the sign of the charge. This is due to the fact that the charge distribution in the water molecule is not symmetric, allowing

Table 2
Position of the first peak and the following minimum of $g_{IO}(r)$ and $g_{IH}(r)$. Also the shell radii and the number of water molecules found in these shells are given

System	q_I/e	g_{IO} r_{max}/Å	g_{IO} r_{min}/Å	g_{IH} r_{max}/Å	g_{IH} r_{min}/Å	Shell radii r_s/Å, r_b/Å	Number of first and second shell members
I	0.0	4.0	5.5	3.8	5.7	4.2 5.5	8.3 13.4
II	0.67	3.45	4.7	3.9	5.2	4.7 5.5	12.5 7.4
III	1.0	3.33	4.1	3.83	4.9	4.0 6.4	8.3 24.0
IV	2.0	3.13	3.9	3.68	4.6	4.0 6.2	12.8 23.5
V	−1.0	3.27	4.0	2.31	3.1	4.0 6.4	8.0 29.3
VI	1.0	3.32	4.1	3.78	4.8	4.0 6.4	8.2 21.9

the positive partial charge a closer approach to his counterion than the negative one.

To classify our "artificial" ions, we may compare the peak positions with experimental ion-water distances. The distance between the Cl^- ion and the nearest neighbour oxygens has been derived by Soper et al. [20] from a neutron diffraction study to be 3.20 Å. The Monte Carlo simulation of Beveridge et al. [25] concerning aqueous solutions of monoatomic ions based on potentials derived from Hartree-Fock calculations, yields a value of 3.2 Å for the maximum position of the ion-center of mass pair correlation function of aqueous Cl^-. Also the other features of their Cl^- distribution function are close to those of our $g_{IO}(r)$ for the anion. All these facts suggest that the anion in the present study may be compared with Cl^-. On the other hand, for Cs^+ an ion-oxygen distance of 3.13 Å was derived from X-ray scattering [36]. That means, our monovalent cation is somewhat larger than Cs^+. Because the same Lennard-Jones σ parameter was also used for the divalent cation, there is no "real" ion which may be compared with it.

Fig. 1 also shows the "running coordination numbers" (scaled by a factor of 0.1) given by

$$n_{IO}(r) = 4\pi\rho_0 \int_0^r s^2 g_{IO}(s)\, ds\,.$$

The number of nearest water molecule neighbours of the ions may be obtained by integrating up to the first minimum which is not very well defined at low ion charges. For the monovalent ions about eight nearest neighbours are found; for the anion slightly less than for the cation. These numbers are within the range discussed in the literature for Cs^+ and Cl^-. In the case of $q_I = +2.0e$ electrostriction yields about 12 nearest neighbours (see also Table 2).

3.1.2. Water-Water Radial Pair Correlation Functions

To investigate the structural differences between bulk water and water in the vicinity of the solute particle a geometric construction of concentric spheres around the ion has been used to distinguish between first and second hydration shells and the bulk. Thus water molecules are classified depending on their ion-oxygen distance r_{IO}:

first shell: $r_{IO} \leq r_s$
second shell: $r_s < r_{IO} \leq r_b$
bulk: $r_b < r_{IO}$

The choice of the parameters r_s and r_b ($r_s < r_b$) is more or less arbitrary but was such that in the case of $q_I \neq 0$ those molecules which establish the first peak in $g_{IO}(r)$ form the first shell. In the case of $q_I = 0.0$ the very broad first peak was subdivided into two shells. The exact r values and the number of water molecules in these shells can be read from Table 2.

In this way the intermolecular atom-atom pair correlation functions about molecules belonging to those three different regions were determined separately. (If in the course of the calculation of these functions both members of a pair of molecules belong to different regions, then the atomic distances arising from such a pair contribute to both $g(r)$-averages.) As an example, Fig. 2 shows the $g_{OH}(r)$ functions which correspond to the first shell and the bulk. The second shell functions have been omitted for clarity. As one can see, the hydration shell function changes its form appreciably when varying the ion charge. In the hydrophobic hydration shell ($q_I = 0.0$) the features of this double peak function are slightly intensified as already observed in an earlier study [5] ("hydration water is more structured than bulk water"), whereas an increasing ion charge destroys more and more its particular shape. The occurring changes are comparable with those caused by an increasing temperature or pressure on pure water.

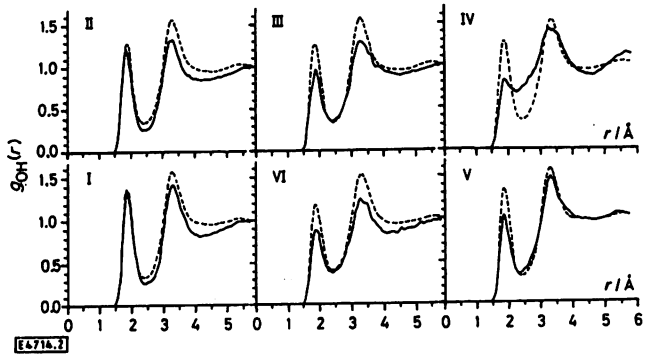

Fig. 2
Intermolecular oxygen-hydrogen pair correlation functions $g_{OH}(r)$ monitoring the difference of water structure in the first hydration shell (full line) compared to the bulk average (dashed line) for the various systems (see also text). Typical water structure is destroyed in the shell with increasing ionic charge

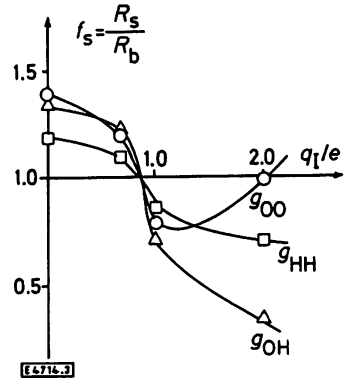

Fig. 3
Variation of the enhancement factor $f_s = R_{\text{first shell}}/R_{\text{bulk}}$ describing the difference in water structure as a function of the cationic charge (syst. I to IV). $f_s > 1$: structure enhancement in the shell, $f_s < 1$: decrease of structure

As a measure of the degree of structure one can take the ratio of the heights of the first maximum and the following minimum $R = g_{max}/g_{min}$. Furthermore, a structure enhancement factor $f_s = R_{shell}/R_{bulk}$ can be defined. If $f_s > 1$ one may say the water structure is increased (comparable to a lowering of temperature), $f_s < 1$ indicates a decrease of structure. In Fig. 3 the variation of the enhancement factor with ion charge is drawn for the cation series (system I to IV, first shell only). As one can see, the structure promoting influence of the uncharged particle is destroyed and reversed with increasing ion charge.

Whereas the structure as described by g_{OH} and g_{HH} is destroyed continuously, the behaviour of $g_{OO}(r)$ indicates a final increase of structure after having passed a minimum. This may be interpreted as follows: intermolecular OH- and HH-correla-

tion is determined mostly by the hydrogen-bond interaction between neighbouring water molecules and is lost with the destruction of the normal water hydrogen bond pattern in the vicinity of the ions. This continuous destruction of hydrogen bond interaction between water molecules also shows up clearly in the pair energy distributions discussed in chapter 4.3. On the other hand a new OO-correlation between hydration-shell water molecules is imposed by the strong packing influence of the highly charged ion, that means, that in this case the oxygen-oxygen correlation is determined mostly by the strong repulsive interaction between these close packed molecules.

Davies et al. [37] report molal shifts of the magnetic resonance for the water protons in aqueous solutions of tetraalkylammonium and alkali metal ions which show at room temperature and below a steady increase with increasing charge/radius ratio, passing from negative (downfield) to positive (upfield) shift. This parallels the present observations which show an increased hydrogen bond structure near the nonpolar solute and a steady destruction of this structure with increasing charge; although in general there are additional effects like the direct influence of the ion on the electron cloud of the hydration water molecules which prohibit a simple relation between nuclear distributions and the chemical shift.

3.1.3. Water-Ion-Water Three Particle Correlation Functions

As we saw in the last two sections, an increasing ion charge leads to a sharpening of the ion-water distribution functions, while on the other hand the typical water-water distributions (mainly $g_{OH}(r)$) are smeared out more and more. The countercurrent trends in these two classes of distribution functions suggest the occurrence of an extremum in the behaviour of those distribution functions which can be considered as combinations of functions belonging to both classes. As an example we consider the frequency distribution of the angle γ which is formed by the oxygen nuclei of two hydration shell water molecules as seen from the ion (see insert of Fig. 5). The distribution shown in Fig. 4 give the probability of finding a pair of hydration shell molecules (both having $r_{IO} \leq r_s = 4.2$ Å) which form an angle with a cosine value between $\cos\gamma$ and $\cos\gamma + \Delta(\cos\gamma)$ with $\Delta(\cos\gamma) = 0.02$. As one can realize from Fig. 4, there is a marked structuring at $q = 0.0$ which vanishes at $q = 1.0e$ and reappears at $q = 2.0e$. The mechanisms which lead to these structures at $q = 0.0$ and $2.0e$, however are of totally different nature.

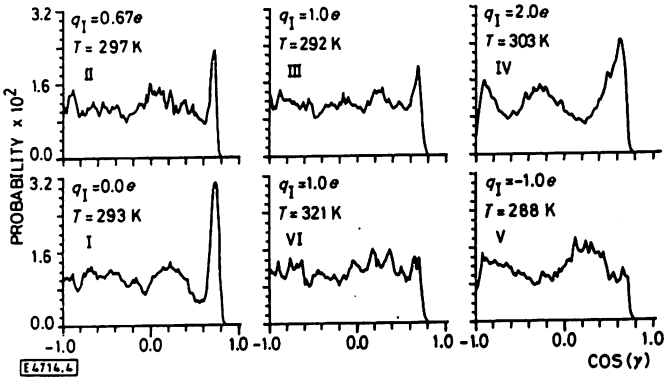

Fig. 4
Probability distribution for the cosine values of angles formed by the oxygen nuclei of two hydration shell water molecules ($r_{IO} \leq 4.2$ Å) as seen from the ion. A minimum of correlation is found near $q_I = 1.0e$

At $q = 0.0$ the occurrence of hydrophobic hydration leeds to clathrate-like water cage fragments (see Ref. [5]), the spatial correlations between hydration water molecules being caused mainly through hydrogen bond interactions. In the case of $q = 2.0e$ the water molecules are strongly attracted by the ion, the hydrogen bonds between the hydration shell molecules are destroyed and a close packing around the ion is obtained. Then the structure at $q = 2.0e$ as seen in Fig. 4 is mainly due to the strong repulsive interaction between the close packed hydration water molecules. In the intermediate region at $q \approx 1.0e$ hydrogen bonding is already disturbed appreciably, but the packing is not yet very effective, which leads to the observed loss of order.

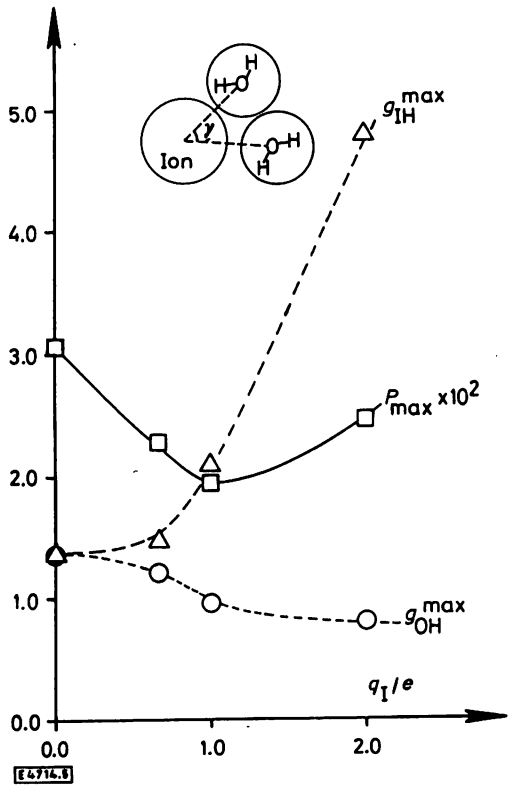

Fig. 5
Maximum probability $P_{max} \cdot 10^2$ (□) from Fig. 4 as a function of cation charge (syst. I to IV) as a measure for the degree of lateral correlation in the hydration shell. The change of the maxima of the IH and OH-pair correlation functions g_{IH}^{max}(△) and g_{OH}^{max}(○) indicate the opposite trends which establish the minimum in P_{max}

In Fig. 5 the maxima P_{max} of the probability distributions in Fig. 4 are drawn as a function of cation charge for the systems near room temperature. If these values are interpreted as a measure for the degree of structuring in the hydration shell, we see that a minimum is reached at about $q_I = 1.0e$. Additionally g_{IH}^{max} and g_{OH}^{max} are indicated as dashed curves to demonstrate the opposite trends which establish the minimum in P_{max}.

The neutral particle function in Fig. 4 shows very clearly its relationship to the water-water pair correlation function $g_{00}(r)$. This seems to justify the superposition approximation used in the hydrophobic effect study of Pratt and Chandler [38], when calculating the three particle probability

$$\rho_{WIW'}(r|r_I, r') \approx \rho_W g_{IW}(|r - r_I|) g_{WW'}(|r - r'|)$$

($\rho_{WIW'}$ is the conditional probability of finding a water molecule W at r, given that a molecule W' is positioned at r' and the solute particle I at r_I). However, as we know from the preceding section and from Ref. [5], one of the essential features of the hydrophobic hydration effect is the change of $g_{WW'}$ in the vicinity of the neutral solute. Thus using $g_{WW'}$ of pure water in the superposition formula is not a good approximation, when studying the hydrophobic effect (e.g. the ratio between the heights of the maximum and the adjacent minimum of the angle distribution is 6.0, the corresponding value for the shell average of $g_{00}(r)$ was found to be 5.9, whereas in the bulk water this value is only 4.2).

As mentioned before, in the case of $q_I = 2.0e$ we have about 12 water molecules in the first hydration shell. This would suggest an icosahedral arrangement of the water molecules around the ion. In that case we would expect large maxima at $\cos\gamma \approx \pm 0.45$ and a small one at $\cos\gamma = -1.0$. As we see from Fig. 4 the observed maxima are appreciably shifted from these values which means that there are large deviations from this most symmetric configuration.

3.2. Orientational Distributions in the First Hydration Shell

It is obvious that different ionic charges will produce different preferential orientations of the hydration shell water molecules. Therefore the orientations of the main molecular fixed vectors (as defined below) with respect to the ion were investigated. In detail, the frequency distributions of the following values have been calculated (M denotes the negative partial charges of the water model, see Fig. 8):

$$\cos\theta = \hat{\mu} \cdot \hat{\mu}_{OI}$$

for

$$\hat{\mu} = \hat{\mu}_{OH} = (r_O - r_H)/|r_O - r_H|,$$

$$\hat{\mu} = \hat{\mu}_{OM} = (r_O - r_M)/|r_O - r_M|$$

and

$$\hat{\mu} = \hat{\mu}_{dip} = (r_M + r_{M'} - 2r_O)/|r_M + r_{M'} - 2r_O|.$$

$$|\cos\theta| = |\hat{\mu} \cdot \hat{\mu}_{OI}|$$

for

$$\hat{\mu} = \hat{\mu}_{HH} = (r_H - r_{H'})/|r_H - r_{H'}|$$

and

$$\hat{\mu} = \hat{\mu}_{MM} = (r_M - r_{M'})/|r_M - r_{M'}|$$

with

$$\hat{\mu}_{OI} = (r_O - r_I)/|r_O - r_I|.$$

The same shell construction as indicated in Table 2 has been used here, with the exception of system I ($q_I = 0$), where the first shell comprises now the total first peak of $g_{IO}(r)$: $r_{\text{first sh.}} = 5.5$ Å, $r_{\text{sec. sh.}} = 7.5$ Å. The sampling interval $\Delta(\cos\theta)$ was 0.04.

As an example we show in Fig. 6 the distributions describing the orientation of $\hat{\mu}_{OH}$. We see that for $q_I = 0$ and for $q_I = 2.0e$ marked structures exist which are totally different in their qualitative appearance and we also recognize that there is a transition region between the two states (near $q_I \approx 0.7e$),

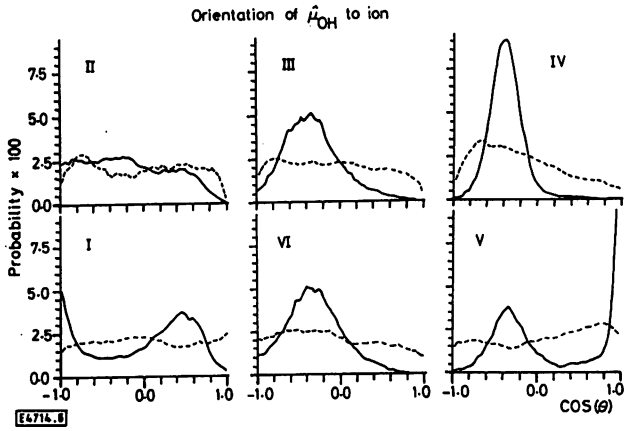

Fig. 6
Distribution functions for the angle cosines describing the OH-bond orientation of water molecules in the first and second hydration shell to the ion (full and dashed lines respectively)

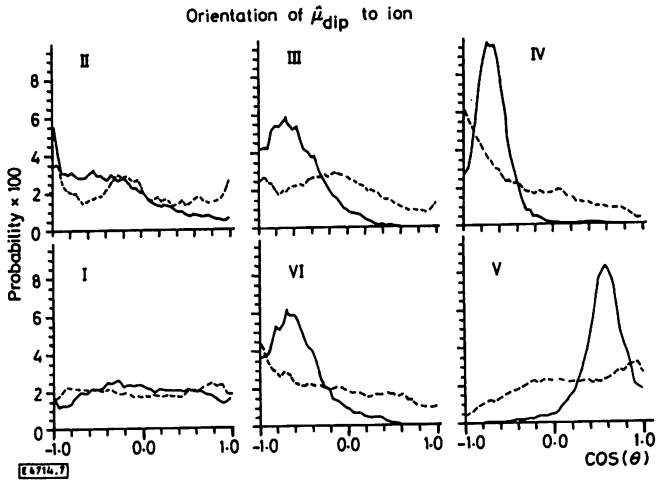

Fig. 7
Distribution functions for the angle cosines describing the electric dipole moment orientation of water molecules in the first and second hydration shell to the ion (full and dashed lines respectively)

where no preferential orientation exists at all (at least for the observed vector). The same is true for $\hat{\mu}_{OM}$. These findings show again a remarkable loss of order in the first hydration shell, when passing from hydrophobic hydration or normal positive ionic hydration to the state of so-called negative hydration. $\hat{\mu}_{dip}$, $\hat{\mu}_{HH}$, and $\hat{\mu}_{MM}$ cannot follow the same pattern, because their distribution functions practically do not show any preferential orientations in the hydrophobic hydration shell at $q_I = 0.0$. Therefore a steady increase of structuring of these functions can be observed with increasing ion charge, although the observed changes are still very weak when proceeding from $q_I = 0.0$ to $q_I = 0.67e$. Fig. 7 shows the dipole orientation as an example. In previous studies Heinzinger et al. [27, 28] also investigated the dipole axis orientation of ST2-water molecules in the vicinity of several ions. Based on these distribution functions (which are comparable to those found here), they could not support the ideas of orientational disordering in the negative hydration shell. But as we see now, a more detailed investigation of the total multidimensional orientational correlation function yields many aspects which support the view

of negative hydration as a state of minimal orientational order between hydrophobic hydration and positive ionic hydration.

The distributions found in the case of $q_I = 0.0$ are totally equivalent to those found in the study of the hydrophobic hydration effect (Ref. [5]). There it was concluded that the water molecules in the first shell are oriented in such a way that one of the four tetrahedral bond directions points radially outward, i.e. away from the center of the spherical solute. The remaining three bond directions straddle the solute particle. The orientational distribution functions for the divalent cation can be interpreted roughly as follows: One of the two negative partial charges points radially to the ion, thus the remaining three bond directions point outward in a tetrahedral angle. A closer look shows that there are slight deviations from perfect tetrahedral orientation. The observed differences can be explained by small tilts of 5 to 8 degrees. The direction of the tilt is such that the electric dipole approaches a radial alignment. In Fig. 8 the averages of the cosine values resp. of the absolute cosine values for the different distributions calculated for the cation series (systems I to IV) are given as functions of the cation charge. At the right side of the diagram those values are indicated which correspond to the ideal tetrahedral orientation as described above. We can see that for several molecule-fixed vectors with increasing cation charge these values are exceeded in the direction of a more radial orientation of the electric dipole. Concerning the anion distribution functions, two facts should be noted: 1. One OH-bond points radially to the ion, forming a linear hydrogen bond. No tilt at all is visible. 2. The

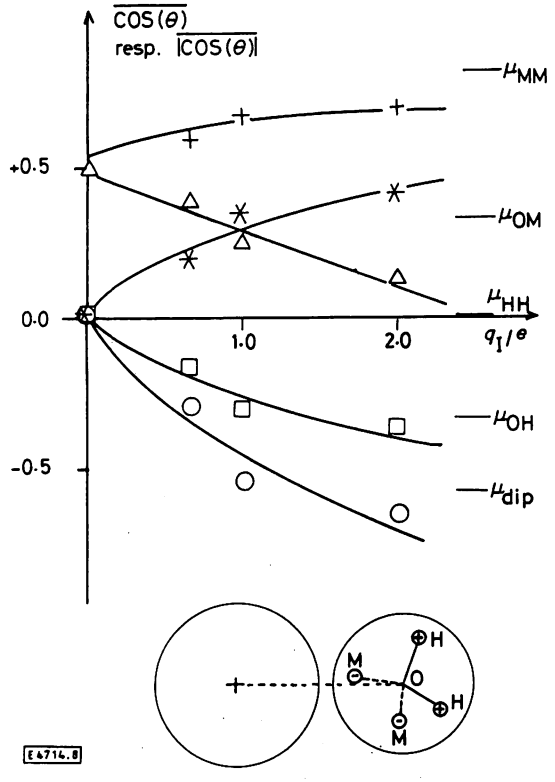

Fig. 8
Averages of the cosine values resp. of the absolute cosine values (see section 3.2) for different distributions calculated for the cation series (syst. I to IV) as a function of the cation charge. Orientation of $\hat{\mu}_{MM}$: +, $\hat{\mu}_{HH}$: △, $\hat{\mu}_{OM}$: *, $\hat{\mu}_{OH}$: □, $\hat{\mu}_{dip}$: ○. At the right hand side values corresponding to ideal tetrahedral orientation are indicated

structuring around the anion is appreciably increased compared to the vicinity of the equivalent cation: the peaks are narrower. This is, as explained before, a consequence of the asymmetric charge distribution in the water molecule.

Finally we want to compare these calculated orientations of hydration water molecules with experimental findings. Concerning the anion hydration shell, there is consensus between many authors: Using X-ray and neutron diffraction methods as well as nuclear magnetic relaxation measurements, a hydrogen-bond orientation was found for F^- [39], Cl^- [20, 40], and I^- [17] which is in agreement with the present results. For cations the same authors find tetrahedral (a lone electron pair pointing to the metal ion), radial dipole, as well as intermediate orientations [17, 20, 40]. Analyzing the orientation of water molecules next to metal ions in a larger number of salt hydrates, Friedman and Lewis [41] find for low charge metal ions mainly tetrahedral orientations; with increasing ion charge the occurrence probability for radial dipole orientations increases. This finding is also in agreement with our discussion of Fig. 8. A clear preference of tetrahedral orientation was also observed in the MD studies of Heinzinger et al. [26]. One may argue that the charge distribution of the ST2 water model overemphasizes this particular configuration, but the interest of the present study on negative hydration effects concentrates mainly on the large qualitative changes of the distribution functions when varying the ionic charge.

4. Energy Calculations

4.1. Hydration Energies

To get a *rough* estimate for the hydration energies in these systems the following procedure has been used. The raw total energy data as given in column 4 of Table 1 have been corrected for the water-water interaction cutoff by using the same method as described in the Appendix of Ref. [3] (Eqs. A4 and A7). For this purpose the orientation correlation factor

$$G_K = \langle M^2 \rangle / N$$

with $M = \sum_{i=1}^{N} \hat{\mu}_i$ had been determined, $\hat{\mu}_i$ is the unit vector along the dipole moment direction for water molecule i. The static dielectric constants ε_0 which are also needed are measured values for "real" water [42]. Thus we finally get the corrected total energy E_{tot}^{corr} given in Table 3. This value refers to N_L (= Avogadro's number) particles (solute + solvent) and is compared with E_{ST2}, the corresponding value of the pure ST2-water system (the same correcting procedure having been applied). These E_{ST2}-values are interpolated for the correct temperature from the total energy data of Ref. [3] and are listed in Table 3. The hydration energy E_{hydr} (in kcal/mol solute) is calculated from the equation

$$216 E_{tot}^{corr} = 215 E_{ST2} + E_{hydr} + \frac{3}{2} kT .$$

Of course, these values have large error bars (of the order of ± 50 kJ/mol), because they are determined as small differences of large corrected quantities. We also know from a number of recent papers that boundary conditions and the interaction cutoff influence the mutual orientation of distant polar molecules strongly [43, 44] and thus also have an appreciable influence on

Table 3
Rough estimate for the hydration energy E_{hydr} and quantities used to derive these values for the different systems

System	q_I/e	$E_{tot}^{uncorr.}$ / kJ mol^{-1}	G_K	ε_0*)	$E_{tot}^{cor.}$ / kJ mol^{-1}	E_{ST2} / kJ mol^{-1}	E_{hydr} / kJ mol^{-1}
I	0.0	−35.13	0.16	80.4	−36.33	−36.19	60
II	0.67	−35.34	0.21	79.0	−36.78	−35.77	250
III	1.0	−36.45	0.17	80.7	−37.67	−36.28	335
IV	2.0	−40.43	0.18	76.5	−41.65	−35.15	1440
V	−1.0	−37.29	0.14	82.1	−38.34	−36.74	380
VI	1.0	−33.52	0.22	70.5	−34.92	−33.43	350

*) From Dorsey (Ref. [42]).

the total energy. On the other hand, the fact that E_{tot} and E_{ST2} have been derived with essentially the same method, systematic errors will cancel out to some measure. The values obtained in this way for the monovalent ions may be compared with single ion hydration energies as given e.g. by Friedman and Krishnan [14] (neglecting volume effects and small temperature differences): $\Delta H^0(Cl^-) = -340$ kJ/mol; $\Delta H^0(Cs^+) = -315$ kJ/mol.

4.2. Water Molecule Binding Energies

The binding energy U_j of a water molecule j is defined as

$$U_j = V_{Ij} + \sum_{\substack{k=1 \\ k \neq j}}^{N_W} V_{jk}$$

where V_{Ij} is the interaction energy between the solute I and the water molecule j (calculated as described in section 2) and V_{jk} is the pair interaction energy between water molecules j and k (the sum over k is restricted to those water molecules within the cut-off radius r_c). In Fig. 9 the average binding energy of the water molecules as a function of the ion-water oxygen distance is shown for the six systems. The horizontal line at the left-hand side indicates the average binding energy of pure ST2 water as derived from Ref. [3] (corrected for the same water interaction cutoff). It is very striking to see that the binding energy is not lowered appreciably in the vicinity of the ion as one would expect when comparing dipole-dipole (water-water) and charge-dipole (ion-water) pair energies. On the contrary, for the structure breaking ions ($q_I = 0.67e$ and $1.0e$) the binding energy of the hydration shell water molecules is even more positive compared to the bulk water. In these hydration shells the strongly attractive ion-water interaction is overcompensated by the loss of at least one hydrogen-bonding possibility and the occurrence of strong water-water repulsions, as will be seen in the next section. The slightly negative deviations in the case of the uncharged solute indicates again the strengthening of hydrogen-bonding in the hydrophobic hydration shell. This generally weak change of water binding energy in the vicinity of the ion was also concluded from infrared absorption measurements [45] and is in total agreement with the predictions of Samoilov [13].

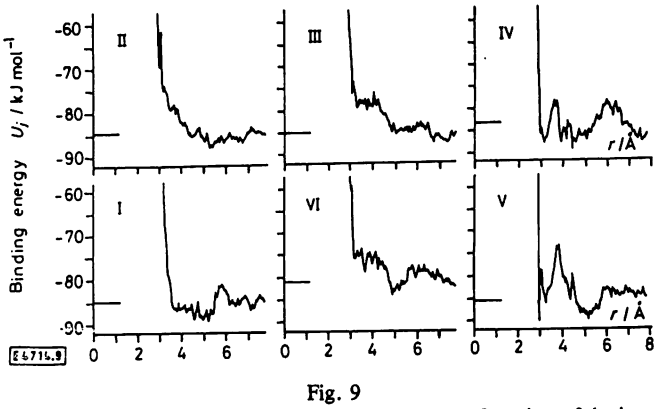

Fig. 9
Average binding energy of the water molecules as a function of the ion-water oxygen distance. The horizontal lines indicate the average binding energy of pure ST2 water as derived from Ref. [3] (corrected for the same water interaction cutoff)

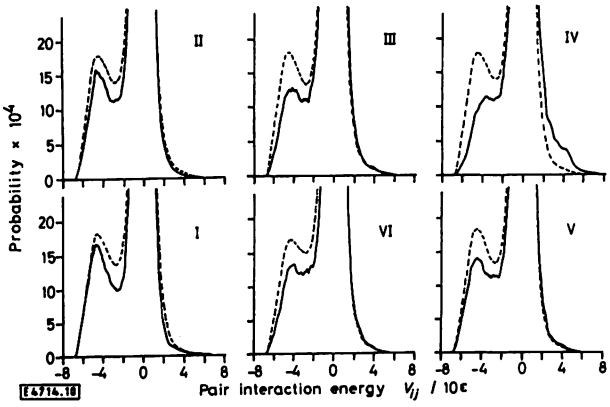

Fig. 10
Occurrence probabilities for the pair interaction energies V_{jk}, monitored separately for bulk and shell water (dashed and full lines). A destruction of typical water hydrogen bond structure with increasing ion charge is indicated. ($\varepsilon = 0.317$ kJ mol^{-1} is the ST2-model Lennard-Jones parameter.)

4.3. Pair Interaction Energy Distributions

As in previous studies [1 − 5] the distribution function for pair interaction energies between two water molecules was calculated. Fig. 10 shows the occurrence probabilities for the pair interaction energies V_{ik}, separately for bulk and shell water. A pair energy V_{ik} is considered in the shell distribution, if one or both members j and k have an ion-oxygen distance $r_{IO} \leq r_s$ ($r_s = 4.4$ Å for system I, $r_s = 4.0$ Å for all other systems), otherwise it is attributed to the bulk distribution (dashed curve). Considering the shell distributions, the shoulder structure on the negative energy side changes appreciably with the ion charge q_I. For $q_I = 0.0$ the shoulder of the shell distribution is slightly more pronounced than in the bulk distribution. This was already observed in Ref. [5] and indicates "more structured" water in the hydrophobic hydration shell. With increasing ion charge this shoulder is more and more flattened out, notifying

destruction of the original water structure, comparable to an increase in temperature or pressure in pure water [2–4]. Thus these distributions show the same behaviour as the water-water radial pair distribution functions discussed in section 3.1.2. The large increase of the distribution function on the positive energy side for $q_i = 2.0e$ (already perceptible at $q_I = 1.0e$) indicates the presence of many strongly repulsive interacting water pairs in the hydration shell, which is due to electrostrictive packing of the hydration water molecules. The overall smaller probabilities in the negative shoulder region of the shell distribution compared to the corresponding bulk values originate from the fact that the neighbouring solute particle excludes other water molecules from close approach [5].

5. Dynamic Properties

5.1. Self-Diffusion

Generally, the "microdynamic structure" of an electrolyte solution has been described in terms of self-diffusion coefficients, residence and reorientation times of the water molecules in various regions around the ions [9]. Within this framework negative hydration is defined by the occurrence of increased self-diffusion coefficients and decreased reorientation times compared to pure water. One of the most interesting and controversal questions is the location of the region of this increased molecular mobility.

According to the Einstein relation the self-diffusion coefficient of the solvent water has been determined from the long time limiting slope of the mean square water oxygen displacement:

$$D = \lim_{t\to\infty} \frac{1}{6t} \langle |r(t + t_0) - r(t_0)|^2 \rangle ,$$

where $r(t)$ is the oxygen coordinate vector of a certain water molecule at time t. According to their position at the starting time t_0 the individual water molecules contribute to different averages:

first shell: $r_{IO}(t_0) < 4.2$ Å
second shell: 4.2 Å $\leq r_{IO}(t_0) < 6.4$ Å
bulk: 6.4 Å $\leq r_{IO}(t_0)$

with $r_{IO}(t_0) = |r_I(t_0) - r(t_0)|$, $r_I(t_0)$ is the position vector of the ion at t_0. The general appearance of these displacement functions is well known from previous studies [1–5]. Table 4 gives the corresponding self-diffusion coefficients derived from these curves by a least square fit (for $t > 0.6$ ps). From the mean-squared deviations of the fit one can estimate on the average relative errors of roughly 5% for D_{bulk}, 10% for $D_{second\ shell}$ and 20% for $D_{first\ shell}$. These errors are mainly due to the different numbers of contributing water molecules to the different averages. Fig. 11 shows the ratios D_{shell}/D_{bulk} for the first and second shell as a function of cationic charge obtained from the near room temperature systems I to IV. As one can see we really get an increased diffusional behaviour in the first hydration shell, if we have an ionic charge of about $2/3e$ to $1e$, at the given ion size. This increase is weaker in the second shell and its occurrence is shifted to higher ionic charges. Near $q_I = 1.5e$ the interpolating curves indicate a behaviour which corresponds to the three region model of Frank and Wen [11]: decreased mobility in the first shell and increased mobility in the second shell. However, it should be noted here that Harris et al. [46] did never find a ratio $D_{second\ shell}/D_{bulk} > 1$ when $D_{first\ shell}/D_{bulk} < 1$.

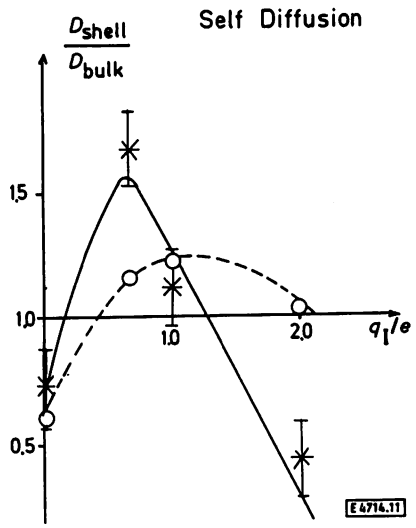

Fig. 11
Ratios D_{shell}/D_{bulk} for the first (*) and second (○) shell water molecules as a function of cationic charge for systems I to IV. An increased mobility in the first hydration shell for charges near $q_I = 1.0e$ is indicated

The magnitude of the increase in mobility in the first shell is in accordance with numbers derived from experimentally obtained self-diffusion coefficients. Hertz et al. [9, 47] calculated ratios D_{shell}/D_{bulk} of 1.1 to 1.2 for Cs^+ and Cl^- (at room temperature) depending on the assumed hydration number.

There is one big discrepancy between the experimental findings and the present simulation runs: The simulation study yields an increased self-diffusion coefficient ratio when increasing the temperature (comparing systems III and VI). This contradicts the experimental observation that an increase in

Table 4
Self-diffusion coefficients derived from mean squared displacements by a least square fit

System	q_I/e	T/°C	D_{bulk} / 10^{-5} cm²/s	$D_{sec.\ shell}$ / 10^{-5} cm²/s	$D_{first\ shell}$ / 10^{-5} cm²/s	$D_{sec.\ shell}/D_{bulk}$	$D_{first\ shell}/D_{bulk}$
I	0.0	20	3.1	2.0	2.3	0.6	0.7
II	0.67	24	3.1	3.5	5.0	1.1	1.6
III	1.0	19	2.9	3.5	3.3	1.2	1.1
IV	2.0	30	3.3	3.4	1.8	1.0	0.5
V	−1.0	15	2.0	2.4	2.8	1.2	1.4
VI	1.0	48	4.4	6.2	8.5	1.4	1.9

temperature reduces the structure breaking ability of the corresponding ions (as we also find it in the next section, when determining reorientation times). Whether this is a consequence of the model, of extreme fluctuations or an indication for an unsufficient equilibration of the high temperature system can only be decided by additional long simulation runs. The absolute values for the bulk water D_{bulk} are roughly 30% higher than the experimental values for pure water at the same temperatures which is in agreement with the pure water simulation runs [3]. This indicates also that the influence of the hydration shell on the bulk average is not very strong.

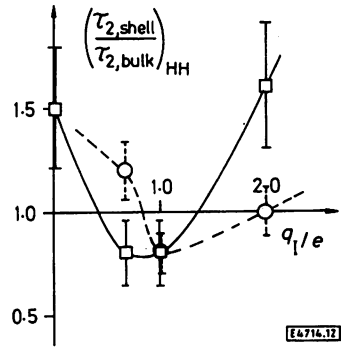

Fig. 12
Ratios τ_{shell}/τ_{bulk} for τ_2 of the proton-proton vector as a function of cationic charge (systems I to IV). □: first shell, ○: second shell

5.2. Reorientational Motion

The increased microscopic mobility of water molecules near structure breaking ions, manifested by decreased reorientation times, was investigated by nuclear magnetic relaxation [9] and dielectric relaxation measurements [10]. Both methods probe the decay of autocorrelation functions $\Gamma_l(t)$ for Legendre Polynomials $P_l(\cos\theta)$ for different molecule-fixed unit vectors $\hat{\mu}_j$:

$$\Gamma_l(t) = \langle P_l(\hat{\mu}_j(t_0) \cdot \hat{\mu}_j(t_0 + t))\rangle .$$

Dielectric relaxation is determined by Γ_1 of the electric dipole direction $\hat{\mu}_{dip}$ (although it has to be kept in mind that dielectric relaxation is a collective process), the intramolecular part of the proton magnetic relaxation by Γ_2 of the proton-proton vector $\hat{\mu}_{HH} = (r_H - r'_H)/|r_H - r'_H|$, the deuterium relaxation in D_2O by $\hat{\mu}_{OH} = (r_O - r_H)/|r_O - r_H|$. The general appearance of these functions is well-known from previous studies [2, 5]: After a short initial period of libration a roughly exponential decay is following. It turns out that in some hydration shells the orientational correlation of the water molecules decays more slowly, in others faster than in the bulk. Correlation times τ_1 and τ_2 (for Γ_1 and Γ_2 respectively) have been calculated by fitting an exponential to the autocorrelation functions, neglecting the librational part (Table 5). For systems II to VI the various averages have been determined in the same way as described in the case of self-diffusion (previous section). For system I only one concentric hydration shell has been constructed, comprising the total first broad peak of $g_{IO}(r)$: $r_{IO}(t_0) < 5.5$ Å (see section 3.1.1).

As an example Fig. 12 shows the ratios τ_{shell}/τ_{bulk} for τ_2 of the proton-proton vector as a function of the ionic charge from system I to IV. It reveals the following remarkable facts:

1. With increasing charge the mobility of the shell molecules passes a maximum (minimum of τ_{shell}/τ_{bulk}) near $q_I = 1.0e$, as already observed in the self-diffusion behaviour. In the minimum region we again find increased mobility in the first hydration shell. From relaxation time measurements Endom et al. [47] found ratios τ_{shell}/τ_{bulk} of 0.7 for Cs^+ and 0.9 for Cl^- at 25 °C, when assuming hydration numbers $n_h^{\pm} = 8$.
2. The interpolating curves in Fig. 12 again suggest that for the present ion size a charge near $q_I = 1.5e$ would produce a microdynamic structure as proposed in the Frank-Wen concentric shell model [11]: decreased mobility in the first shell and increased mobility in the second shell. But at $q_I = 2/3e$ even the opposite hydration model is observed: a more mobile first shell is surrounding by a more rigid second shell. In a graphical picture one may say that the originally rigid hydrophobic hydration shell is "softened" from the interior, when adding increasing charges and finally "stiffened" again when the charges become larger.

With the exception of system IV (comprising the divalent ion), the absolute values of $\tau_{2,bulk}$ are about 30% smaller than pure water values derived from Krynicki's [48] proton magnetic relaxation time measurements (and assuming $\tau_2 = 2.5$ ps for 25 °C [9]). For the pure model liquid van Gunsteren et al. [34] determined reorientation times which are even shorter (1.5 ps at 299 K), but this may be a consequence of their very small interaction cutoff. In system IV $\tau_{2,bulk}$ shows a much weaker deviation from experimental values which can be explained by a perceptible influence of the large ionic charge beyond the second hydration shell (increasing τ). Ratios τ_1/τ_2 have also been determined. For pure Brownian rotational diffusion one expects $\tau_1/\tau_2 = 3$, but as in Ref. [5] it was found that there are deviations from this value which are small for the dipole axis and stronger for the proton-proton vector. Finally, comparing the reorientation correlation times of the systems III and VI it can be seen very clearly that the structure breaking influence of the monovalent ion vanishes with increasing temperature. As mentioned in the previous section this is expected from experimental observations [9].

Table 5
Correlation times τ_1 and τ_2 obtained by exponential fits of the reorientation autocorrelation functions

System	τ_2 of $\hat{\mu}_{HH}$ in ps			τ_2 of $\hat{\mu}_{OH}$ in ps			τ_1 of $\hat{\mu}_{dip}$ in ps		
	bulk	sec. sh.	first sh.	bulk	sec. sh.	first sh.	bulk	sec. sh.	first sh.
I	1.9	–	2.9	1.9	–	2.6	4.6	–	6.5
II	1.9	2.3	1.6	1.8	2.3	2.0	4.6	5.8	4.0
III	2.0	1.6	1.6	2.0	1.8	1.6	4.6	4.0	5.7
IV	2.0	1.9	3.2	2.0	1.9	2.7	5.2	4.7	6.4
V	2.6	1.7	2.1	2.6	1.7	1.7	5.8	3.7	3.2
VI	1.2	1.2	1.2	1.1	1.1	1.3	2.8	3.0	2.8

In principle it is possible to estimate from this temperature dependence an activation energy E for the reorientation process, using the elementary kinetic formula

$$\tau = \tau_0 \exp(E/RT) .$$

Using τ_1 and τ_2 (bulk average) for β_{dip}, β_{HH}, and β_{OH} one finds values within the range $E = 13.5 \pm 2.0$ kJ/mol which is close to the number 13.8 kJ/mol derived from n.m.r. measurements of pure water for the temperature region 35 to 80°C [9]. Of course, this method is not very accurate, because we have only two temperature points and can hardly be applied to the hydration shells. But averaging over both shells and over the values for τ_1 and τ_2 we find mean values $E = 15.9$ kJ/mol for β_{dip}, 10.9 kJ/mol for β_{OH} and 8.8 kJ/mol for β_{HH} (Endom et al. [49] from n.m.r. measurements claim $E = 11.3$ kJ/mol for the rotational motion in the hydration sphere of Cs^+). This indicates anisotropic reorientation in the vicinity of the ion. Therefore, in a final calculation time correlation functions Γ_1 and Γ_2 for the first hydration shell molecules have been determined separately for vectors with different initial orientations (at time t_0) with respect to the ion. As we can see from Fig. 6 the orientational distribution for β_{OH} has two distinct peaks for systems I and V. The same is true for β_{OM} with respect to the cation in the other systems. The calculations show that in systems IV and V β_{OM} respectively β_{OH} which belong initially to the peak near $\cos\theta = +1$ (pointing to the ion) clearly reorient more slowly than the corresponding second vector in the same molecule which contributes to the peak near -0.33 (on the average the reorientation times differ by a factor of 1.6). In the other systems the reorientation times are equal within 25%. Anisotropic reorientation of the hydration shell molecules had also been concluded from nuclear magnetic relaxation time measurements for aqueous solutions of Li^+ [49].

6. Conclusions

As mentioned previously Engel and Hertz [8] determined the ratio of the water molecule reorientation times τ_{shell}/τ_{bulk} for many different ions. In Fig. 19 of Ref. [8] these authors plotted essentially this ratio versus the ionic radius r. For constant ionic charge they obtained curves with a form similar to a parabola. The minima of the monovalent cation and anion series are located at slightly larger radius values than those of Cs^+ and I^-, respectively. To explain this behaviour Engel and Hertz derived a formula which relates τ_{shell}/τ_{bulk} to the electric field produced by the ion in its hydration shell (which is proportional to the "surface charge" of the ion: $q_I/4\pi r_I^2$). If these considerations are valid a comparable curve should also be obtained when it would be possible to vary the ionic charge at constant ionic radius. This has been done in the present model experiment and the results (see e.g. Fig. 12) confirm this idea very well. Although a fixed Lennard-Jones radius σ, as applied in this study, does not really guarantee a fixed "ionic radius" because an increasing ionic charge also changes e.g. the distance of the zero transitions of the ion-water pair interaction potential. But this effect should be small compared to the charge effect.

There have been other authors which related various properties of ions in solution to the ionic charge or radius, e.g. Conway [50] observed thermodynamic functions like partial molar volume and entropy of hydration or the dielectric decrement of various salts in aqueous solution and found indications for the occurrence of an extremum when plotting these quantities versus the ionic radius. Paquette and Jolicoeur [51] find a comparable behaviour when making the same plots for standard enthalpies of transfer (from H_2O to D_2O), "structural temperature shift" from IR measurements and solvent isotope effect on the ionic Walden product for the same cation series as Conway. As has been stated previously by Millero [52], for different properties the extremum occurs at slightly different surface charges. This can also be seen in the present results, e.g. when comparing Figs. 6 and 4. The minimum of orientational order of the water OH-bonds occurs near $q_I = +2/3e$, whereas the minimum of three particle correlation (Fig. 4) is closer to $q_I = +1.0e$. As a consequence in an extreme case an ion may behave "structure breaking" when looking at one property and "structure promoting" for another property.

It is generally agreed that anions and cations of comparable size and equal magnitude of charge show different solvation strength. This can be explained as a consequence of the unsymmetric charge and mass distribution in the water molecule. But certainly there are also problems originating from the separation of measured properties into single ion contributions, which includes in many cases some arbitrariness. In the present study comparing systems III and V the hydration of the anion is stronger compared to the cation, when looking e.g. at the ion-water radial pair correlation function (ratio $g_{IW}^{max}/g_{IW}^{min}$) or the dipole orientation distribution (Fig. 7). These differences cannot be attributed to the small temperature difference between the two systems but can be explained by the fact that the positive partial charge of the ST2 model can approach the anion closer than the negative partial charge to the cation. On the other hand, the microdynamic behaviour of the water molecules in the vicinity of the anion is not slowed down compared to the cation.

As has been stated previously in connection with comparable simulation studies [6] one should notice that there are still some fundamental problems in simulating water due to boundary conditions, the potential model, convergence characteristics etc. These are discussed in several recent publications [34, 44, 53]. Some justifications, why this method can be used nevertheless have been given in section 2. It should also be noticed here that Rahman and Stillinger [3] observed the density maximum for the ST2 water at about +27°C. This indicates the uncertainties of the model when studying the influence of temperature on more subtle structural effects and suggests that the structural changes observed in the present study should be compared to "real" aqueous systems at temperatures markedly below room temperature.

Finally it should be mentioned that a short computer movie has been produced, showing the vicinity of the solute particle during sections of roughly 1 ps for systems I to IV. In the case of $q_I = 0.0$ the solute particle oscillates with large amplitude in a roomy cage which leads to the observed broad ion-water pair correlation functions (Fig. 1). At $q_I = 2.0e$ the ion is surrounded tightly by its hydration water molecules, only very small amplitude-higher frequency motions are possible. Changes in preferential orientation and microscopic mobility can also be observed.

Summarizing, the major results of this study are:

1. An increasing surface charge of the solutes destroys continuously the structure of the water as existing in the pure liquid or in the hydrophobic hydration shell, comparable to an increasing applied external pressure.
2. With increasing ionic charge a maximum of disorder and mobility in the hydration shell is passed. This is a consequence of the competition between the water-water and ion-water interactions.
3. Ionic hydration models which include the possibility that the region of structure breaking may extend up to the surface of the ion, are supported.

This work is part of a project supported by a grant of the Deutsche Forschungsgemeinschaft to Prof. H. G. Hertz. His encouragement and his many helpful comments are appreciated. The simulation program used in this study is based on a pure water version kindly provided by Dr. A. Rahman, Argonne National Laboratory, USA.

References

[1] A. Rahman and F. H. Stillinger, J. Chem. Phys. *55*, 3336 (1971).
[2] F. H. Stillinger and A. Rahman, J. Chem. Phys. *57*, 1281 (1972).
[3] F. H. Stillinger and A. Rahman, J. Chem. Phys. *60*, 1545 (1974).
[4] F. H. Stillinger and A. Rahman, J. Chem. Phys. *61*, 4973 (1974).
[5] A. Geiger, A. Rahman, and F. H. Stillinger, J. Chem. Phys. *70*, 263 (1979).
[6] C. Pangali, M. Rao, and B. J. Berne, J. Chem. Phys. *71*, 2982 (1979).
[7] V. G. Dashevsky and G. M. Sarkisov, Mol. Phys. *27*, 1271 (1974); J. C. Owicki and H. A. Scheraga, J. Am. Chem. Soc. *99*, 7413 (1977); A. Swaminathan, S. W. Harrison, and D. L. Beveridge, J. Am. Chem. Soc. *100*, 5705 (1978); S. Okazaki, K. Nakanishi, H. Touhara, and Y. Adachi, J. Chem. Phys. *71*, 2421 (1979); G. Alagona and A. Tani, J. Chem. Phys. *72*, 580 (1980).
[8] G. Engel and H. G. Hertz, Ber. Bunsenges. Phys. Chem. *72*, 808 (1968).
[9] H. G. Hertz, in: Water, a Comprehensive Treatise, ed. by F. Franks, Vol. 3, Chap. 7, Plenum, New York 1973.
[10] R. Pottel, in: Water, a Comprehensive Treatise, ed. by F. Franks, Vol. 3, Chap. 8, Plenum, New York 1973.
[11] H. S. Frank and W. Y. Wen, Discuss. Faraday Soc. *24*, 133 (1957).
[12] R. W. Gurney, Ionic Processes in Solution, McGraw Hill, New York 1953.
[13] O. Y. Samoilov, Discuss. Faraday Soc. *24*, 141 (1957); O. Y. Samoilov, Structure of Aqueous Electrolyte Solutions and the Hydration of Ions, Consultants Bureau, Enterpr. Inc., New York 1965.
[14] H. L. Friedman and C. V. Krishnan, in: Water, a Comprehensive Treatise, ed. by F. Franks, Vol. 3, Chap. 1, Plenum, New York 1973.
[15] H. G. Hertz, Ber. Bunsenges. Phys. Chem. *68*, 907 (1964).
[16] F. H. Stillinger and A. Ben-Naim, J. Phys. Chem. *73*, 900 (1969).
[17] A. Geiger and H. G. Hertz, J. Solution Chem. *5*, 365 (1976); H. Langer and H. G. Hertz, Ber. Bunsenges. Phys. Chem. *81*, 478 (1977).
[18] F. Franks, in: Water, a Comprehensive Treatise, ed. by F. Franks, Vol. 4, Chap. 1, Plenum, New York 1974.
[19] H. G. Hertz, Ber. Bunsenges. Phys. Chem. *77*, 531 (1973).
[20] A. K. Soper, G. W. Neilson, J. E. Enderby, and R. A. Howe, J. Phys. C *10*, 1793 (1977); G. W. Neilson and J. E. Enderby, J. Phys. C *11*, L625 (1978).
[21] E. Kálmán and G. Pálinkás, Z. Phys. Chem. (Leipzig) *259*, 609 (1978).
[22] E. Clementi, Liquid Water Structure, Springer Verlag, Berlin 1976.
[23] R. O. Watts and I. J. McGee, Liquid State Chemical Physics, Wiley, New York 1976.
[24] M. R. Mruzik, F. F. Abraham, D. E. Schreiber, and G. M. Pound, J. Chem. Phys. *64*, 481 (1976).
[25] D. L. Beveridge, M. Mezei, S. Swaminathan, and S. W. Harrison, in: Computer Simulation of Bulk Matter from a Molecular Perspective, ed. by P. G. Lykos, ACS Symposium Series, 1978.
[26] A. Rahman, in: Report of Workshop on Ionic Liquids, Centre Européen de Calcul Atomique et Moléculaire, Orsay, France 1974.
[27] K. Heinzinger and P. C. Vogel, Z. Naturforsch. *29a*, 1164 (1974).
[28] P. Bopp, W. Dietz, and K. Heinzinger, Z. Naturforsch. *34a*, 1424 (1979), and literature cited therein.
[29] C. L. Briant and J. J. Burton, J. Chem. Phys. *64*, 2888 (1976).
[30] R. O. Watts, in: Water, a Comprehensive Treatise, ed. by F. Franks, Vol. 6, Chap. 6, Plenum, New York 1979.
[31] H. M. Lin and R. L. Robinson, Jr., J. Chem. Phys. *54*, 52 (1971).
[32] M. V. Bobetic and J. A. Barker, J. Chem. Phys. *64*, 2367 (1976).
[33] A. Rahman, F. H. Stillinger, and H. L. Lemberg, J. Chem. Phys. *63*, 5223 (1975).
[34] W. F. van Gunsteren, H. J. Berendsen, and J. A. C. Rullmann, Faraday Discuss. *66*, 6614 (1978).
[35] J. P. Ryckaert, G. Ciccotti, and H. J. Berendsen, J. Comput. Phys. *23*, 327 (1977).
[36] H. Bertagnolli, J.-U. Weidner, and H. W. Zimmermann, Ber. Bunsenges. Phys. Chem. *78*, 2 (1974).
[37] J. Davies, S. Ormondroyd, and M. C. R. Symons, J. Chem. Soc., Faraday Trans. II, *68*, 686 (1972).
[38] L. R. Pratt and D. Chandler, J. Chem. Phys. *67*, 3683 (1977).
[39] H. G. Hertz and C. Rädle, Ber. Bunsenges. Phys. Chem. *77*, 521 (1973).
[40] A. H. Narten, F. Vaslow, and H. A. Levy, J. Chem. Phys. *58*, 5017 (1973).
[41] H. L. Friedman and L. Lewis, J. Solution Chem. *5*, 445 (1976).
[42] N. E. Dorsey, Properties of Ordinary Water-Substance, Hafner Publishing Company, New York 1968.
[43] A. J. C. Ladd, Mol. Phys. *33*, 1039 (1977).
[44] M. Neumann and O. Steinhauser, Mol. Phys. *39*, 437 (1980).
[45] W. A. P. Luck, Progr. Colloid Polym. Sci. *65*, 6 (1978).
[46] K. R. Harris, H. G. Hertz, and R. Mills, J. Chim. Phys. *75*, 39 (1978).
[47] L. Endom, H. G. Hertz, B. Thül, and M. D. Zeidler, Ber. Bunsenges. Phys. Chem. *71*, 1008 (1967).
[48] K. Krynicki, Physica *32*, 167 (1966).
[49] H. G. Hertz, R. Tutsch, and H. Versmold, Ber. Bunsenges. Phys. Chem. *75*, 1177 (1971).
[50] B. E. Conway, J. Solution Chem. *7*, 721 (1978).
[51] J . Paquette and C. Jolicoeur, J. Solution Chem. *6*, 403 (1977).
[52] D. E. Millero, in: Water and Aqueous Solutions, ed. by R. A. Horne, Wiley-Interscience, New York 1972.
[53] M. Mezei, S. Swaminathan, and D. L. Beveridge, J. Chem. Phys. *71*, 3366 (1979).

(Eingegangen am 31. Juli 1980, endgültige Fassung am 13. Oktober 1980) E 4714